On the Numerical Solution of Unsteady Fluid Flow Problems by a Meshless Method

Tonino Sophy — Hamou Sadat

Laboratoire d'Études Thermiques (UMR 6608)
ESIP
40 avenue du Recteur Pineau,
86022 Poitiers cedex

{sophy, sadat}@let.ensma.fr

ABSTRACT. *A diffuse approximation method for the solution of time-dependent Navier-Stokes equations is presented. Different preconditioned iterative methods for solving the pressure correction equation are tested. Sample results are presented for the window cavity problem and the fluid flow around a circular cylinder.*

RÉSUMÉ. *On présente une méthode de résolution des équations de Navier-Stokes instationnaires par approximation diffuse. Une comparaison de différentes méthodes itératives de résolution de l'équation de correction de pression est effectuée. Quelques résultats obtenus dans les cas de la convection naturelle dans une cavité différentiellement chauffée et de l'écoulement à l'aval d'un obstacle cylindrique sont donnés.*

KEYWORDS: *Meshless method, diffuse approximation, unsteady fluid flow.*

MOTS-CLÉS : *Méthode meshless, approximation diffuse, écoulements instationnaires.*

REEF – 11/2002. Meshfree Computational Mechanics, pages 989 to 1004

1. Introduction

In spite of the great success of the finite element method as an effective numerical method for the solution of partial differential equations on complex domains, there has been a growing interest in meshless methods over the last years [ALU 01, BEL 94, CHA 01, LIU 01, OSH 01, ZHA 00]. For our part, we have developed a diffuse approximation based collocation method for solving incompressible steady fluid flows [SAD 95, SAD 96]. One of the primary issues in these problems, whether a regular or unstructured type grid is used, is how to handle the pressure-velocity coupling. This is an important issue since an explicit equation for the pressure does not exist. The pressure-velocity coupling problem can be avoided by using a streamfunction-vorticity approach. In this case, we have shown that the diffuse approximation method is as accurate as the well known control-volume based finite element method [PRA 98]. However streamfunction-vorticity methods are not readily extended to three dimensions. Therefore, the method has been extended to the primitive variables formulation of the Navier-Stokes equations by means of a projection algorithm [COU 98]. The Poisson equation that arises from the pressure correction process consumes however a large portion of the computational time.

Since the memory resource in many cases is limited for large-scale problems, direct methods are seldom used and iterative schemes are preferred. The conjugate gradient algorithm is a very powerful method for solving symetric positive definite sparse linear systems, especially when it is used with a preconditioner. In this algorithm, the residual vector is mimized in each iteration step with respect to some suitable norm. During the process, the residual vectors are constructed in such a way that they are orthogonal to each other with regard to the Euclidian inner product. Additionally, because of the symmetry of the matrix, the residual vectors fulfill a three-term recursion, which is a characteristic of the algorithm. However, this algorithm fails in general for nonsymetric or indefinite linear systems. Several attempts have then been made to come up with a generalization of this method for the nonsymmetric case. One can for example maintain the minimization property by choosing the direction vector as a linear combination of the residual vector and k previous direction vectors. This approach has been used in methods like Orthomin, Orthodir and other generalized conjugate gradient schemes. The generalized minimal residual type algorithms (GMRES, FGMRES, DQGMRES) are theoretically equivalent and more robust approaches. One can also maintain the three-term recursion property. This is done by the biconjugate gradient type algorithms (BCG, BICGSTAB, DBCG).

The aim of the present article is to discuss the application of the diffuse approximation based collocation method to unsteady fluid flows. In the following sections, the general method of solution is described. Some numerical results obtained by using different preconditioned iterative methods are then given. Two test problems are finally presented. The first one is the laminar natural convection in a differentially heated square cavity. The second test case is the oscillatory flow past a circular cylinder.

All numerical simulations have been conducted on a PC computer with 256MB of main memory.

2. The diffuse approximation based collocation method

Description of the method

Let $\Phi : R^n \rightarrow R$ be a scalar field whose values Φ_i are known at the points $\mathbf{x}_i$ of a given set of N nodes in the studied domain $D \in R^n$. The diffuse approximation gives estimates of Φ and its derivatives up to the order k at any point $\mathbf{x} \in D$. The Taylor expansion of Φ at $\mathbf{x}$ is estimated by a weighted least squares method which uses only the values of Φ at some points $\mathbf{x}_i$ situated in the vicinity of $\mathbf{x}$.

It can thus be written:

$$\Phi_i^{\,estimated} = \mathbf{p}(\mathbf{x}_i - \mathbf{x}).\boldsymbol{\alpha}^{\mathrm{T}}(\mathbf{x}) \tag{1}$$

where $\mathbf{p}(\mathbf{x}_i\text{-}\mathbf{x})$ is a line vector of polynomial basis functions and $\boldsymbol{\alpha}(\mathbf{x})$ a vector of coefficients which are determined by minimizing the quantity:

$$I(\alpha) = \sum_{i=1}^{N} \omega(\mathbf{x}, \mathbf{x}_i - \mathbf{x})\left[\Phi_i - \mathbf{p}(\mathbf{x}_i - \mathbf{x}).\boldsymbol{\alpha}^{\mathrm{T}}(\mathbf{x})\right]^2 \tag{2}$$

in which ω is a weight-function of compact support, equal to unity at this point, decreasing when the distance to the node increases and zero outside a given domain of influence (a more precise description of ω will be done next).

Minimization of equation (2) then gives:

$$\mathbf{A}(\mathbf{x})\boldsymbol{\alpha}(\mathbf{x}) = \mathbf{B}(\mathbf{x}) \tag{3}$$

where:

$$\mathbf{A}(\mathbf{x}) = \sum_{i=1}^{N} \omega(\mathbf{x}, \mathbf{x}_i - \mathbf{x})\,\mathbf{p}^{\mathrm{T}}(\mathbf{x}_i - \mathbf{x})\,\mathbf{p}\;\;(\mathbf{x}_i - \mathbf{x}) \tag{4}$$

$$\mathbf{B}(\mathbf{x}) = \sum_{i=1}^{N} \omega(\mathbf{x}, \mathbf{x}_i - \mathbf{x})\,\mathbf{p}^{\mathrm{T}}(\mathbf{x}_i - \mathbf{x})\Phi_i \tag{5}$$

In fact **A**(**x**) is the sum of only n'(**x**) matrix of rank 1, n'(**x**) being the number of nodes influencing **x**. By inverting system (3), one obtains the components of α which are the derivatives of Φ at **x** in terms of the neighboring nodal values Φ_i. In this work, the Taylor expansion is truncated at order 2. The polynomial vector used is

$$\mathbf{p}(\mathbf{x}_i - \mathbf{x}) = \left\langle 1, (x_i - x), (y_i - y), \frac{(x_i - x)^2}{2}, (x_i - x)\cdot(y_\mathrm{i} - y), \frac{(y_i - y)^2}{2} \right\rangle \qquad (6)$$

and

$$\langle \alpha_1, \alpha_2, \alpha_3, \alpha_4, \alpha_5, \alpha_6 \rangle = \langle \Phi, \frac{\partial \Phi}{\partial x}, \frac{\partial \Phi}{\partial y}, \frac{\partial^2 \Phi}{\partial x^2}, \frac{\partial \Phi^2}{\partial x \partial y}, \frac{\partial^2 \Phi}{\partial y^2} \rangle \qquad (7)$$

Then, the following system is obtained:

$$\begin{Bmatrix} \varphi \\ \dfrac{\partial \varphi}{\partial x} \\ \dfrac{\partial \varphi}{\partial y} \\ \dfrac{\partial^2 \varphi}{\partial x^2} \\ \dfrac{\partial^2 \varphi}{\partial x \partial y} \\ \dfrac{\partial^2 \varphi}{\partial y^2} \end{Bmatrix} = A(X)^{-1} . \left\{ \sum_{i=1}^{n'(X)} \omega(X, X_i - X) . \langle P(X_i - X) \rangle^T \cdot \Phi_i \right\} \qquad (8)$$

The square matrix **A**(**x**) is not singular as long as the number n'(**x**) of the connected nodes at a given point is at least equal to the size of α and are not colinear or cocircular [DEM 84, BRE 02].

In our studies, several weight-functions were tried and it was found that the following Gaussian window (figure 1):

$$\begin{aligned} &\omega(\mathbf{x}, \mathbf{x}_i - \mathbf{x}) = \exp\left[-3\ln(10) \cdot \left(\frac{|\mathbf{x}_i - \mathbf{x}|}{\sigma} \right)^2 \right] \\ &\omega(\mathbf{x}, \mathbf{x}_i - \mathbf{x}) = 0 \quad \text{if } (\mathbf{x}_i - \mathbf{x})^2 > \sigma^2 \end{aligned} \qquad (9)$$

behaves rather well. The distance of influence σ is updated at each point in order to use at least 9 neighbors in the approximation.

The previous approximation is then used in a point collocation method to solve partial derivatives equations. At each point of the discretization, the derivatives appearing in the equation to be solved are replaced by their diffuse approximation thus leading to an algebraic system that is solved after the introduction of the Dirichlet boundary conditions. The Neumann boundary conditions on the other hand are replaced by their diffuse approximation and then introduced in the algebraic system as described in [SAD 95, SAD 00, SOP 02].

3. The pressure correction equation

In the primitive variable formulation, the incompressible Navier-Stokes equations (for natural convection problems) can be written as follows [SAD 00]:

$$\frac{\partial \mathbf{v}}{\partial t} + \mathbf{v} \cdot \nabla \mathbf{v} = \frac{\mathrm{Pr}}{\sqrt{\mathrm{Ra}}} \nabla^2 \mathbf{v} - \nabla p + \frac{\mathbf{g}}{g} \mathrm{Pr}\, \theta \tag{10}$$

$$\nabla \cdot \mathbf{v} = 0 \tag{11}$$

$$\frac{\partial \theta}{\partial t} + \mathbf{v} \nabla \theta = \frac{1}{\sqrt{\mathrm{Ra}}} \nabla^2 \theta\,. \tag{12}$$

where Pr and Ra are the Prandtl and the Rayleigh numbers respectively, and g is the gravitational acceleration.

Although the pressure gradient term appears in the momentum equation, there is no apparent equation to solve for the pressure. Therefore, special techniques are required. The SIMPLE algorithm [PAT 80] and its various versions and the projection algorithm [COM 82] have been generally used.

These methods are essentially iterative guess-and-correct procedures. They consist of solving the momentum equation by using a guessed pressure field to obtain an intermediate velocity field. The pressure correction equation, which is obtained by using the continuity equation, is then solved using the intermediate velocity. The process is continued until the convergence test is satisfied.

In this work, we used an equal order projection algorithm, which is described below.

3.1. *Projection algorithm*

The basic methodology of our projection algorithm in the case of bidimensional natural convection can be summarized as follows:

1. Initialization of the fields $(u,v,p,\theta)^{i}$.
2. Resolution of momentum equations for estimated velocities u^{*} and v^{*}.

$$\frac{u*}{\Delta\tau}-\frac{\Pr}{\mathrm{Ra}^{1/2}}\left(\frac{\partial^2 u*}{\partial x^2}+\frac{\partial^2 u*}{\partial y^2}\right)+u^{\mathrm{i}}\,\frac{\partial u*}{\partial x}+v^{i}\,\frac{\partial u*}{\partial y}=\frac{u^{\mathrm{i}}}{\Delta\tau}-\frac{\partial p^{i}}{\partial x} \tag{13}$$

$$\frac{v*}{\Delta\tau}-\frac{\Pr}{\mathrm{Ra}^{1/2}}\left(\frac{\partial^2 v*}{\partial x^2}+\frac{\partial^2 v*}{\partial y^2}\right)+u^{\mathrm{i}}\,\frac{\partial v*}{\partial x}+v^{i}\,\frac{\partial v*}{\partial y}=\frac{v^{\mathrm{i}}}{\Delta\tau}-\frac{\partial p^{\,i}}{\partial y}+\Pr\theta^{i} \tag{14}$$

3. Resolution of pressure correction equation

$$\frac{\partial^2\ p'}{\partial x^2}+\frac{\partial^2\ p'}{\partial y^2}=\frac{1}{\Delta\,\tau}\left(\frac{\partial u*}{\partial x}+\frac{\partial v*}{\partial y}\right) \tag{15}$$

where the boundary condition is:

$$\frac{\partial p'}{\partial \mathbf{n}}=0$$

on a wall.

4. Calculation of the correcting component of the velocities.

$$\begin{aligned} u' &= -\frac{\partial p'}{\partial x}\cdot\Delta\tau \\ v' &= -\frac{\partial p'}{\partial y}\cdot\Delta\tau \end{aligned} \tag{16}$$

5. Correction of the fields

$$\begin{aligned} p^{i+1} &= p^{i} + p' \\ u^{i+1} &= u^{*} + u' \\ v^{i+1} &= v^{*} + v' \end{aligned} \tag{17}$$

6. Resolution of energy equation.

$$\frac{\theta^{i+1}}{\Delta\tau}+u^{i+1}\frac{\partial\theta^{i+1}}{\partial x}+v^{i+1}\frac{\partial\theta^{i+1}}{\partial y}-\frac{1}{\mathrm{Ra}^{1/2}}\left(\frac{\partial^2\theta^{i+1}}{\partial x^2}+\frac{\partial^2\theta^{i+1}}{\partial y^2}\right)=\frac{\theta^i}{\Delta\tau} \tag{18}$$

7. Check for convergence. If the convergence criterion is not respected, we jump to the second step.

3.2. *Discretization of the pressure correction equation*

During the projection algorithm process, the pressure correction equation (15) is written in its matrix form as follows:

$$\mathbf{Mp'}=\mathbf{b} \tag{19}$$

where p' and b are not to be confused with the previous definitions. The matrix **M** is built line by line using equation (8). If $\langle a_l \rangle$ is the lth line of the matrix $\mathbf{A}(\mathbf{x})^{-1}$, and k is the number of the line corresponding to the node $\mathbf{x}_k$ then we have :

$$\mathbf{M}(k,i)=\omega(\mathbf{x}_k,\mathbf{x}_i-\mathbf{x}_k).\left(\langle a_4\rangle+\langle a_6\rangle\right)\cdot\mathbf{p}(\mathbf{x}_i-\mathbf{x}_k) \tag{20}$$

and

$$\mathbf{b}(k)=\frac{1}{\Delta\tau}\left[\sum_{i=1}^{n'(\mathbf{x}_k)}\omega(\mathbf{x}_k,\mathbf{x}_i-\mathbf{x}_k)\cdot\left(\langle a_2\rangle\cdot u_i^*+\langle a_3\rangle\cdot v_i^*\right)\cdot\mathbf{p}(\mathbf{x}_i-\mathbf{x}_k)^{\mathrm{T}}\right] \tag{21}$$

where u^* and v^* are the estimated values of the velocity.

The gaussian weight function used in this work is shown on figure 1. Let us consider now, the situation depicted on figure 2 where the node M_i is localized on a boundary, and where M_k is a neighboring node of M_i. During the discretization process at M_k the node M_i is not involved whereas the implementation of the Neumann type boundary condition at the node M_i involves the node M_k. This leads to an asymmetrical matrix, even if the non-symmetric element number is very low compared to the total number of elements. This leads to a slow convergence of the iterative algorithm.

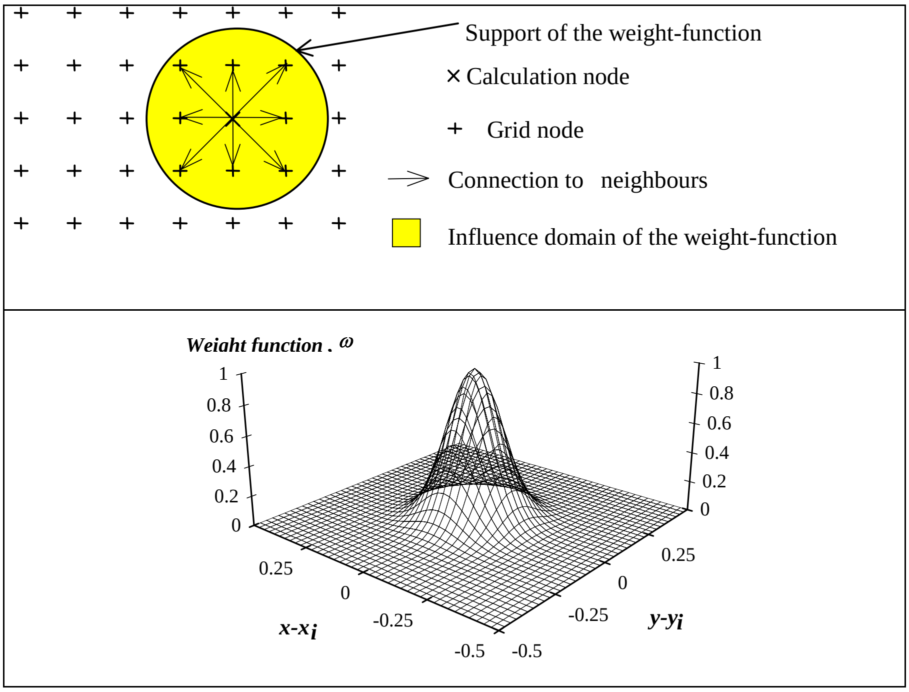

Figure 1. *Neighboring nodes and gaussian weight function*

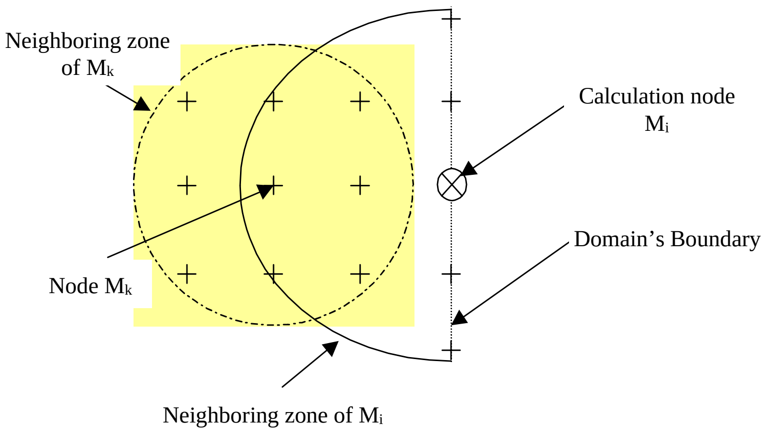

Figure 2. *Boundary nodes and their neighbours*

4. Performance evaluation of iterative methods

One of the important properties of CG-like methods is the so-called super linear convergence behaviour. The convergence rate improves as the iteration proceeds. In many cases, the initial convergence can be very irregular and slow. Therefore, the high asymptotic convergence rate may not be so desirable if the early stage convergence is slow or unstable. This motivates this study to investigate the early stage convergence behaviour of various CG-like methods when applied to find the numerical solution of the pressure correction system that arises in our projection algorithm.

The following methods were tested with the pressure correction equation matrix obtained in the differentially heated square cavity problem:

– Bi-Conjugate Gradient (BCG)
– Bi-Conjugate Gradient with partial Pivoting (DBCG)
– Conjugate Gradient for Normal Residual Equation (CGNR)
– Bi-Conjugate Gradient Stabilized (BCGSTAB)
– Transpose-Free Quasi-Minimum Residual method (TFQMR)
– Generalized Minimum Residual (GMRES)
– Flexible version of GMRES (FGMRES)
– Direct Quasi-GMRES (DQGMRES)
– Full Orthogonal Method (FOM)

and the results are given in the following section.

A description of these methods can be found elsewhere [SAA 96]. It is well known that the use of a preconditioner improves considerably the convergence process. One of the most used technique is the incomplete LU factorization with different fill levels ILU(k). We can also mention the modified incomplete LU factorization, MILU(k). In this work, we have chosen the ILUT(k) preconditioner which was implemented as suggested by Saad [SAA 96]. Two parameters corresponding to the number of elements kept on each line of the matrix (excepting the diagonal values), and the value under which elements are ignored, are respectively set to (lfil=15) and (droptol=10^{-4}).

4.1. *Problem description*

The test problem originates from the simulation of laminar natural convection in a differentially heated square cavity (figure 3a). In this problem, the fluid reaches a steady state flow for a wide range of Rayleigh number (up to 10^8). At a critical value around Ra=1.8.10^8, the system undergoes a first bifurcation to a pseudo periodic solution. We have thus chosen to test the different algorithms at a Rayleigh number of 10^8 whose solution is depicted on figure 3b.

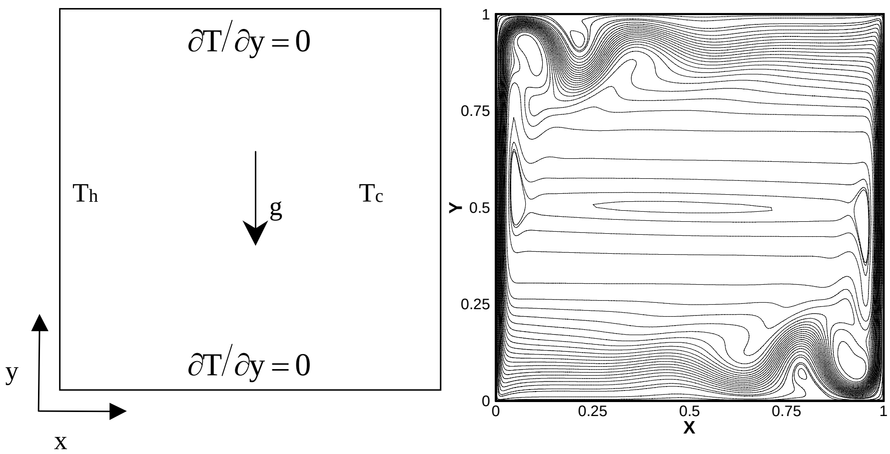

(a) (b)

Figure 3. *(a) Differentially heated square cavity (b) Streamlines for Ra=10^8*

The domain is dicretized with different irregular grids (from 41×41 up to 201×201). In the x,y plane, the non uniform grids obeyed the law:

$$\begin{pmatrix} x \\ y \end{pmatrix} = \frac{1}{2}\left\{1 + \frac{\tanh\left(2\begin{pmatrix} x_r \\ y_r \end{pmatrix} - 1\right)}{\tanh(1)}\right\} \tag{22}$$

where the variables x_r, y_r change within [0,1] and are uniformly distributed. The choice of a finer grid near the walls is motivated by the need to improve the solution in the boundary layers. The time step is fixed to 2.10^{-2} for all the simulations.

4.2. *Results*

In this section, we present some results obtained by using the pressure matrix equation at the first iteration of the first time step. The maximum number of iterations has been fixed to 1000 for all the grids used except for the 201×201 grid for which a number of 3000 has been used. If the maximum number of iterations is reached, the iterative solver stops and returns the appropriate warning. The vector **b** used in equation (19) is set in order to obtain a unity vector solution (so the error can be easily estimated).

The convergence criterion is defined as follow:

$$\left\|\mathbf{A}\mathbf{x}_i - \mathbf{b}\right\| \leq rtol \cdot \left\|\mathbf{A}\mathbf{x}_1 - \mathbf{b}\right\| + atol \tag{23}$$

where *rtol*, *atol* are two parameters that are fixed for each case, and $\mathbf{x}_1$, $\mathbf{x}_i$ are approached solutions at the first and at the ith iteration. Five different cases are considered during this study (table1).

The iteration number necessary to reach the convergence criterion and the residual norm $(\left\|\mathbf{A}\mathbf{x} - \mathbf{b}\right\|)$ are given in table 2 for each case.

Table 1. *Description of test cases*

	Ra	Grid	*rtol*	*atol*
Case 1	10^8	81×81	10^{-10}	0
Case 2	10^8	41×41	10^{-10}	0
Case 3	10^8	41×41	0	10^{-6}
Case 4	10^8	201×201	10^{-10}	0
Case 5	10^8	201×201	0	10^{-6}

Table 2. *Convergence results*

	Case 1		Case 2			
Method	Iteration number	Residual norm	Iteration number	Residual norm		
Bcg	68	$1.61.10^{-7}$	34	$1.32.10^{-7}$		
Dbcg	69	$1.61.10^{-7}$	35	$1.32.10^{-7}$		
-		-	810	$4.6.10^{-7}$		
47		$1.29.10^{-6}$	22	$3.4.10^{-7}$		
Tfqmr	57	$4.42.10^{-7}$	26	$1.18.10^{-7}$		
Gmres	107	$1.81.10^{-6}$	18	$5.62.10^{-8}$		
Fgmres	107	$1.81.10^{-6}$	18	$5.62.10^{-8}$		
Dqgmres	74	$1.7.10^{-6}$	18	$5.62.10^{-8}$		
Fom	92	$1.35.10^{-6}$	18	$5.62.10^{-8}$		
	Case 3		Case 4		Case 5	
Méthod	Iteration number	Residual norm	Iteration number	Residual norm	Iteration number	Residual norm
Bcg	32	$1.29.10^{-7}$	178	$1.16.10^{-5}$	186	$4.85.10^{-7}$
Dbcg	33	$1.19.10^{-7}$	201	$1.19.10^{-5}$	231	$2.76.10^{-7}$
Cgnr	799	$8.15.10^{-7}$	-	-	-	-
Bcgstab	21	$3.4.10^{-7}$	139	$5.1.10^{-6}$	143	$6.37.10^{-7}$
Tfqmr	25	$1.25.10^{-7}$	205	$1.11.10^{-6}$	207	$5.32.10^{-7}$

Gmres	16	$7.01.10^{-7}$	1056	$1.46.10^{-5}$	1245	$9.13.10^{-7}$
Fgmres	" "	" "	1000	$1.46.10^{-5}$	1207	$9.2.10^{-7}$
Dqgmres	" "	" "	876	$1.42.10^{-5}$	929	$8.93.10^{-7}$
Fom	" "	$7.04.10^{-7}$	1018	$1.31.10^{-5}$	1255	$9.28.10^{-7}$

It can be seen that the CGNR algorithm is very slow whenever it converges, while BCG and DBCG algorithms have similar comportment for all the treated cases. Concerning GMRES type methods and FOM, one can see that they are faster for low order systems (41×41 grid). For the 81×81 and the 201×201 grids, BCGSTAB and TFQMR appear to be more efficient (BCGSTAB being the fastest).

Although it is not among the aims of the present article to study the problem of transition to non steady flow for the cavity problem, it is useful to point out that an unsteady solution has been found at $Ra=2.10^8$ using a 201×201 mesh. We found a fundamental frequency of 0.0518, which is in close agreement with the findings (f=0.0522) of Janssen *et al.* [JAN 93]. The time evolution of the velocity at (x=0.5;y=0.5) is finally depicted on figure 4.

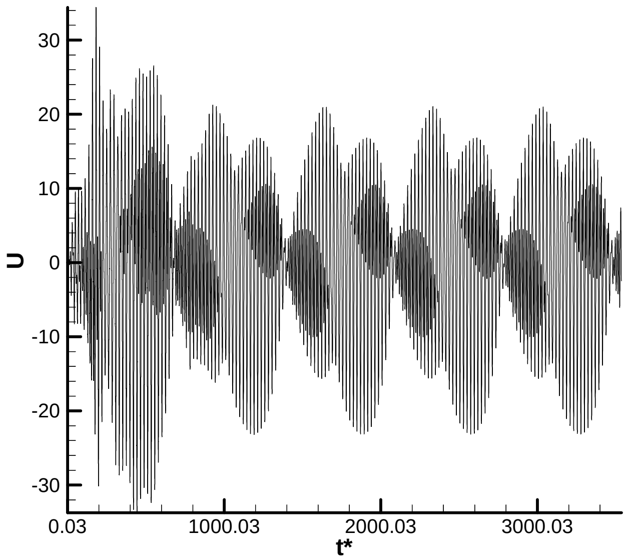

Figure 4. *Time evolution of the horizontal velocity at point (x=0.5, y=0.5)*

5. Flow around a circular cylinder

The fluid flow past a circular cylinder is the second case considered. The problem description and boundary conditions are shown on figure 5.

The flow has a steady state solution composed of two contrarotative vortexes for Reynolds numbers up to Re≈35. Above this critical Reynolds number, the two cells start to oscillate and lengthen successively, making a fluid detachment at a frequency f related the Strouhal number $\left(St = {f.D}/{U_\infty} \right)$.

The flow has been simulated for a Reynolds number Re=65 with a 30 000 nodes irregular grid and an adimensional time step Δτ=0.02. The calculated Strouhal number St=0.155 compares very well with the results of Saiki et al. [SAI 96] who found St=0.152 with a 64 000 nodes grid and a virtual boundary method. The streamlines over a period are shown on figure 6.

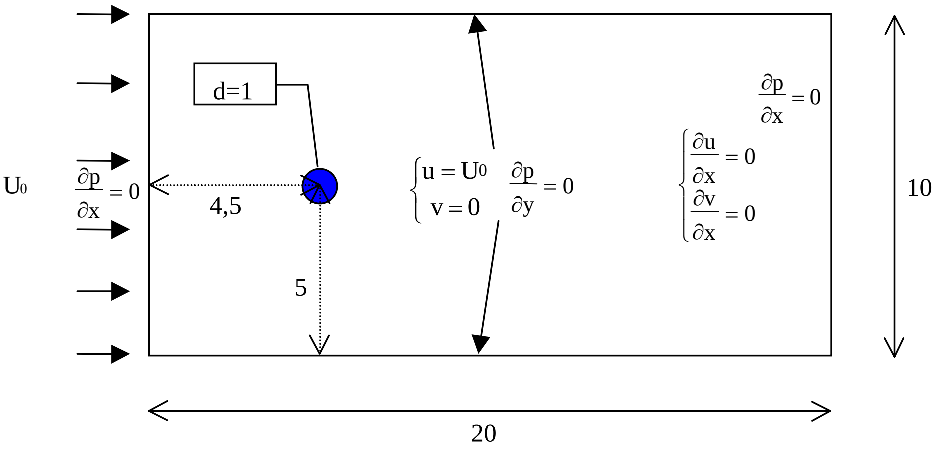

Figure 5. *Description of the cylinder problem*

6. Conclusion

A diffuse approximation method for solving unsteady incompressible fluid flow problems has been presented. It was demonstrated that preconditioned BICGSTAB is a suitable method for the solution of the pressure correction equation. As shown by the comparison with existing numerical solutions, results are very accurate in both space and time. We have not discussed here the problem of essential boundary conditions which remains still an open question. Further work is still needed in that direction.

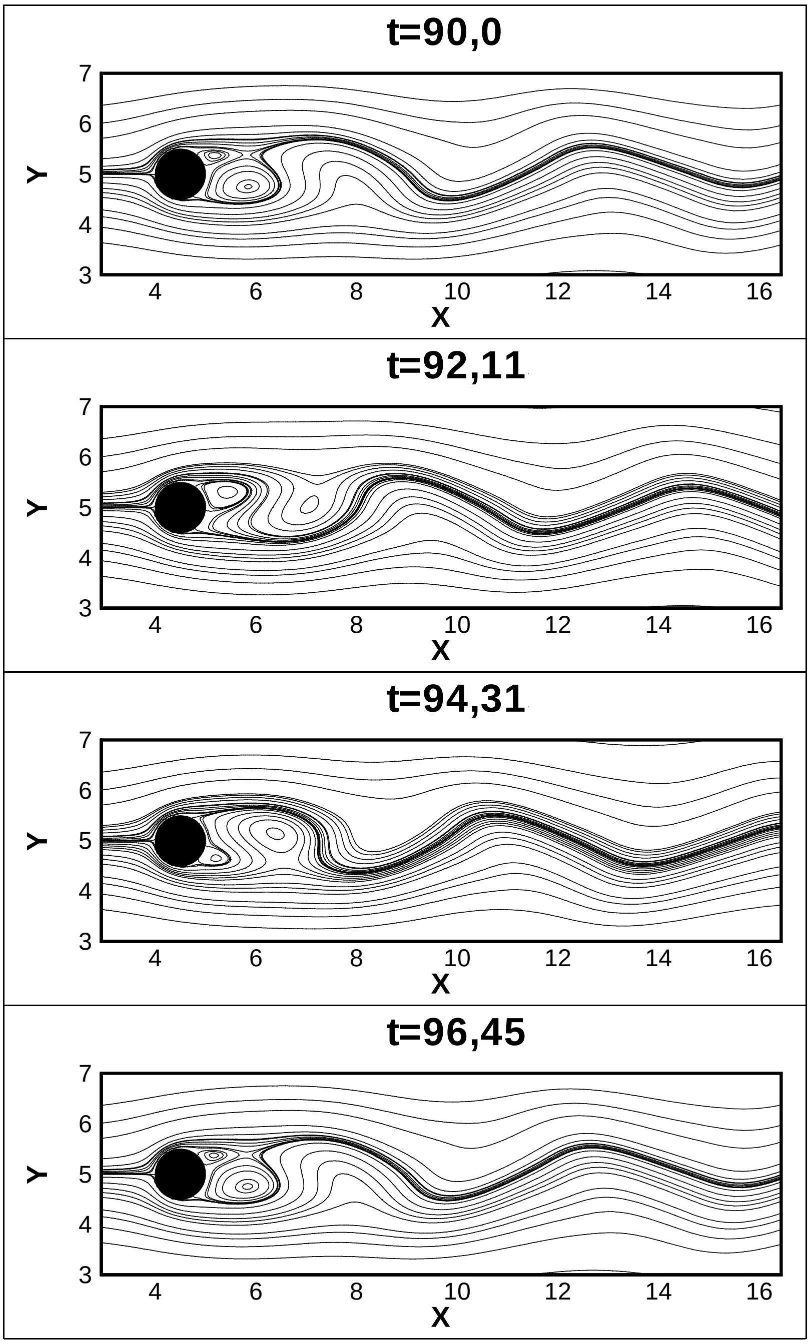

Figure 6. *Streamlines over a period for Re=65*

7. References

[ALU 01] ALURU N. R., LI G., « Finite cloud method: A true meshless technique based on fixed reproducing Kernel », *International Journal for Numerical Methods in Engineering*, Vol. 50, 2001, pp. 2373-2410.

[BEL 94] BELYTSCHKO T., LU YY., GU L., « Element-free Galerkin methods », *International Journal for Numerical Methods in Engineering*, Vol. 37, 1994, pp. 229-256.

[BRE 02] BREITKOPF P., RASSINEUX A. and VILLON P., « An introduction to the moving least squares meshfree methods », *Revue Européenne des Éléments Finis*, No 7-8, 2002.

[CHA 01] CHATI M. K., PAULINO G. H., MUKHERJEE S., « The meshless standard and hypersingular boundary node methods-Applications to error estimation and adaptivity in the three-dimensional problems », *International Journal for Numerical Methods in Engineering*, Vol. 50, 2001, pp. 2233-2269.

[COM 82] COMINI G. and DEL GIUDICE S., « Finite element solution of the incompressible Navier-Stokes equations », *Num. Heat Transfer*, Vol. 5, 1982, pp. 463-478.

[COU 98] COUTURIER S., SADAT H., « Résolution des équations de Navier-Stokes dans la formulation en variables primitives par approximation diffuse », *C. R. Acad. Sciences*, t. 326, série IIb, 1998, pp. 117-119.

[DEM 84] DEMKOWICZ L., KARAFIAT A. and LISZKA T., « On some convergence results for FDM with irregular mesh », *Comp. Methods Appl. Mech. Engrg.*, Vol. 42, 1984, pp. 343-355.

[JAN 93] JANSSEN R. J. A., HENKES R. A. W. M., « Accuracy of finite-volume discretizations for bifurcating natural-convection flow in a square cavity », *Numerical Heat Tranfer*, Part B, Vol. 24, 1993, pp. 191-207.

[LIU 01] LIU G. R., GU Y. T., « Local point interpolation method for stress analysis of two-dimensional solids », *Structural Engineering and Mechanics*, Vol. 11, 2001, pp. 221-236.

[OHS 01] OHS R. R., ALURU N. R., « Meshless analysis of piezoelectric devices », *Computational Mechanics*, Vol. 27, 2001, pp. 23-36.

[PAT 80] PATANKAR S. V., *Numerical Heat Transfer and Fluid Flow*, Hemisphere, Washington, DC 1980.

[PRA 98] PRAX C., SALAGNAC P. and SADAT H., « Diffuse approximation method and control volume based finite element methods : a comparative study », *Num. Heat Transfer*, Part B, Vol. 34, 1998, pp. 303-321.

[SAA 96] SAAD Y., « *Iterative methods for Sparse linear system* », PWS, Boston, MA.

[SAD 95] SADAT H., PRAX C., « Résolution des problèmes de mécanique des fluides et de thermique par approximation diffuse », *Congrès de la Société Française des Thermiciens*, Poitiers, mai 1995.

[SAD 96] SADAT S., PRAX C., SALAGNAC P., « Diffuse approximation method for solving natural convection in porous media », *Transport in Porous Media*, Vol 22, num. 2, 1996, pp. 215-223.

[SAD 00] SADAT H. and COUTURIER S., « Performance and accuracy of a meshless method for laminar natural convection », *Numer. Heat Transfer, Part B Fundamentals*, Vol. 37, 2000, pp. 455-467.

[SAI 96] SAIKI E. M., BIRINGEN S., « Numerical simulation of a cylinder in uniform flow: Application of a virtual boundary method », *J. Comput. Phys.*, Vol. 123, 1996, pp. 450-465.

[SOP 02] SOPHY T., SADAT H., PRAX C., « A meshless formulation fir three-dimensional laminar natural convection », *Num. Heat Transfer, Part B Fundamentals*, Vol. 41, 2002, pp. 433-445.

[ZHA 00] ZHANG X., SONG K. Z., LU M. W., LIU X., « Meshless methods based on collocation with radial basis functions », *Computational Mechanics*, Vol. 26, 2000, pp. 333-343.